coatings

MDPI

Article

Influence of Heating Conditions for Formation of a Thin Apatite Film on Zirconia Using a Molecular Precursor Method

Masatsugu Hirota [1,*], Chihiro Mochizuki [2], Mitsunobu Sato [3] and Tohru Hayakawa [1]

1 Department of Dental Engineering, Tsurumi University School of Dental Medicine, 2-1-3 Tsurumi, Tsurumi-ku, Kanagawa, Yokohama 230-8501, Japan; hayakawa-t@tsurumi-u.ac.jp
2 Division of Liberal Arts, Kogakuin University, 1-24-2 Nishi-shinjuku, Shinjuku-ku, Tokyo 163-8677, Japan; mochizukic@cc.kogakuin.ac.jp
3 Department of Applied Physics, School of Advanced Engineering, Kogakuin University, 1-24-2 Nishi-shinjuku, Shinjuku-ku, Tokyo 163-8677, Japan; lccsato@cc.kogakuin.ac.jp
* Correspondence: hirota-masatsugu@tsurumi-u.ac.jp; Tel.: +81-45-580-8369

Academic Editor: Alessandro Lavacchi
Received: 7 February 2017; Accepted: 26 April 2017; Published: 9 May 2017

Abstract: The influence of heating conditions, heating temperature, and heating time on the formation of a thin carbonate-containing hydroxyapatite (CA) film onto partially stabilized zirconia using a molecular precursor method was evaluated. The molecular precursor solution was prepared from a mixture of calcium-ethylenediaminetetraacetic acid complex and phosphate compounds at Ca/P ratio of 1.67. After the application of molecular precursor solution onto zirconia, four different heating conditions—namely, 600 °C-2 h, 800 °C-2 h, 1000 °C-2 h, and 600 °C-4 h—were applied. No distinct difference of surface appearance of CA coating was observed between 600 and 800 °C-2 h. Fusion of apatite crystals was observed at 1000 °C-2 h. Surface roughness of CA film at 1000 °C-2 h was significantly higher than those under other heating conditions. Heating at 800 °C produced a significantly more hydrophilic surface and higher degree of crystallization. No significant differences were recognized in the critical load at the first crack in the coating among the four samples by scratch tests. After 30 days' immersion in phosphate buffered saline, the four different CA coating films were still present. Simulated body fluid immersion experiments were performed as in vitro biocompatibility tests. After 48 h immersion, the CA film at 800 °C-2 h showed a greater amount of spherical crystal precipitation. It was suggested that properties of CA coating on partially stabilized zirconia using a molecular precursor method were influenced by the heating temperature and time.

Keywords: zirconia; apatite; molecular precursor method; dental implant; simulated body fluid; scratch test

1. Introduction

In implant dentistry, titanium implants have been used because of their high biocompatibility and excellent mechanical properties. Yttria-stabilized tetragonal zirconia polycrystal (Y-TZP) has recently become an attractive alternative to titanium [1,2]. Some of the advantages of Y-TZP dental implants include esthetic performance due to the non-metal color, high mechanical strength, fracture toughness, low plaque adhesion, and applicability of CAD/CAM processing systems in dentistry [3–5].

Direct structural and functional connection between bone and the surface of a titanium implant is called osseointegration [6]. In the case of Y-TZP as a dental implant, clear evidence of osseointegration is still controversial. Hoffmann et al. [7] reported that Y-TZP implants had a slightly higher degree of bone apposition than titanium implants two weeks after implantation in femoral condyles of rabbits. However, bone apposition was higher in titanium implants than in Y-TZP at 4 weeks.

A significant difference was also observed in the removal torque between titanium and Y-TZP implants at 12 weeks [8]. Surface modification of Y-TZP implants may be needed to obtain reliable osseointegration. Among the options, apatite coating is a useful method to improve the bone response of Y-TZP implants. Our previous study achieved a thin and uniform carbonate-containing hydroxyapatite (CA) film coating of less than 1 μm on Y-TZP using a molecular precursor method [9]. The progress of apatite deposition on CA coated Y-TZP after immersion in simulated body fluid (SBF) and a larger amount of new bone formation and higher bone-to-implant contact (BIC) ratio of CA coated Y-TZP were observed by implantation in rabbits.

The molecular precursor method [10,11] is an apatite coating technique. Molecular precursor solution is an ethanol solution of EDTA-calcium complex and phosphate compound. A thin and adherent apatite film was obtained by applying molecular precursor solution on the material surface and treating with heat. The resulting apatite was CA. This process is very simple and inexpensive compared to physical vapor deposition methods such as magnetron sputtering or plasma spraying.

As the molecular precursor method is a wet process, it is possible to coat any complex shapes. Hayakawa et al. and Amemiya et al. processed CA coating on not only the surface but also the inside of a three-dimensional titanium fiber structure [12,13]. Takahashi et al. [11] investigated the influence of heating temperature on the fabrication of CA coating on titanium. They examined the crystal structure of CA coating at heating temperatures of 300, 400, 500, 600, and 700 °C. Below 500 °C, the amorphous phase of CA coating was dominant and few crystal structures of CA coating were identified. At heating temperatures of 600 and 700 °C, a higher degree of crystallinity of CA coating was obtained. However, heat treatment above 700 °C seemed to cause a phase transition of titanium [14]. They concluded that a heating temperature of 600 °C is suitable for producing an adherent CA film on titanium. Our previous study employed a heating temperature at 600 °C according to the results for titanium [9]. However, Y-TZP is more stable than titanium at temperatures higher than 600–700 °C. A higher heating temperature and longer heating time should result in higher crystallinity of the CA coating.

In the present study, we investigated the influence of heating conditions, temperature and time, on the properties of CA film coating on Y-TZP. The null hypothesis tested was that a higher heating temperature and longer heating time would produce greater adherence and higher crystallinity of the CA coating on Y-TZP.

2. Materials and Methods

2.1. Zirconia Substrate

Yttria (3 mol %) stabilized tetragonal zirconia polycrystal disks (Y-TZP; TZ-3YB-E, 12 mm in diameter and 1 mm in thickness, Tosoh, Tokyo, Japan) were used. After polishing with abrasive paper (#1200), polished disks were ultrasonically cleaned in ethanol and distilled water.

2.2. Apatite Coating Using the Molecular Precursor Method

Y-TZP was coated with CA film using the molecular precursor method as previously described [11]. The molecular precursor solution was adjusted in three steps as shown in Figure 1. Briefly, step 1: Preparation of a calcium-EDTA/amine ethanol solution; step 2: Preparation of dibutylammonium diphosphate salt ($(((C_4H_9)_2NH_2)_2P_2O_6 \cdot 2H_2O)$); step 3: Preparation of the molecular precursor solution by adding dibutylammonium diphosphate salt to calcium-EDTA/amine ethanol solution with an adjustment of Ca/P to 1.67 (calcium ion concentration = 0.25 mmol/g).

25 μL of molecular precursor solution was dropped on each Y-TZP disk surface and spin-coated in double step mode at 500 rpm for 5 s and 2000 rpm for 30 s using a spin coater (1H-D7; MIKASA, Tokyo, Japan) [9,11]. After the application of molecular precursor solution onto Y-TZP, the Y-TZP sample was heated at one of four heating conditions, namely, 600 °C-2 h, 800 °C-2 h, 1000 °C-2 h and 600 °C-4 h. Heat treatment was performed using a tubular furnace (EPKPO12-K; ISUZU, Niigata,

Japan) under oxygen gas introduction at a rate of 100 mL/min. The specimens for any measurements were all from different batches.

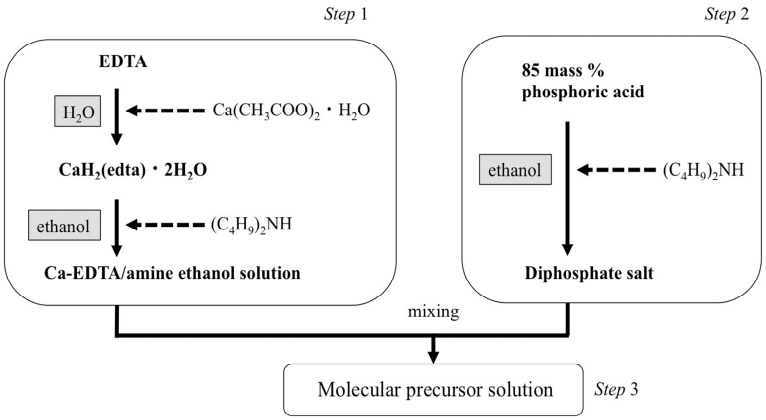

Figure 1. Preparation steps for the molecular precursor solution.

2.3. Morphology and Surface Roughness

The surface morphology after CA coating was observed by scanning electron microscope (SEM; JSM-5600LV, JOEL, Tokyo, Japan). The specimens were sputter-coated with Au and observed at an accelerating voltage of 15 kV.

Three-dimensional surface topography of the CA coating on Y-TZP was observed using an atomic force microscope (AFM; Nanosurf Easyscan 2, Nanosurf AG, Gräubernstrasse, Switzerland) in tapping mode (cantilever: TapAl-G, Budget sensors, Bulgaria; resonance frequency: 190 kHz, spring constant: 48 N/m). The arithmetic average of the roughness profile (R_a) and average roughness of three-dimensional surface (S_a) were calculated within the 2.5 μm × 2.5 μm square areas of AFM images. Five measurements were performed for each specimen.

2.4. Surface Wettability

The surface wettability of the specimens was characterized by contact angle measurement with respect to 0.5 μL double distilled water using an Auto Contact Angle Meter and attached analysis system (DMe-201 and FAMAS, Kyowa Interface Science, Saitama, Japan). Ten measurements of 3 s each were made for each condition, and all analyses were performed at the same temperature and humidity. In addition, uncoated Y-TZP was measured as a reference.

2.5. Crystal Structure of CA Coating

The crystal structure of coated CA thin films on Y-TZP disks was characterized by X-ray diffraction (XRD; SmartLab, Rigaku, Tokyo, Japan) with a thin layer attachment (incidence angle θ = 0.3°), which had an X-ray source of CuKα, and power of 45 kV × 200 mA. Measurements were performed three times.

2.6. Adhesiveness of CA Coating Films

The scratch adhesion test [15] was performed on coated disks using the diamond-stylus scratch method (Nano Scratch Tester, Anton Paar, Graz, Austria). A diamond stylus (rockwell type, tip radius: 10 μm) was moved over each specimen surface with a linearly increasing load until failure occurred at critical loads. Some scratch test parameters were established as follows: Begin to end load was 3 to 1000 mN, and speed of moving stage was 1.5 mm/min (length: 1.5 mm). L_c value was defined as the critical load at the first crack in the coating. Scratch tests were performed in three places for each sample and L_c values were calculated. A number of the specimens was three.

2.7. Durability of CA Coating

Y-TZP disks after CA coating were immersed in 20 mL of phosphate buffered saline (PBS) solution with pH = 7.4 in a polypropylene bottle for 1, 7, or 30 days at 37 °C. After the immersion, the disks were dried in a desiccator. The presence of CA films was observed by SEM at an accelerating voltage of 15 kV.

2.8. SBF Immersion

Hanks' balanced salt solution (HBSS) without organic species was employed as SBF [16]. Concentrations of HBSS are listed in Table 1. Y-TZP disks after CA coating were immersed in 20 mL of HBSS with an adjusted pH to 7.4 at 37 °C in a polypropylene bottle. The medium and bottles were replaced after 24 h to expose the disks to fresh medium. After immersion for 24 or 48 h, the disks were immediately dried in a desiccator. The surface appearances of Y-TZP disks after immersion in HBSS were observed using SEM at an accelerating voltage of 15 kV.

Table 1. Concentrations of electrolytes in HBSS.

Ion	Concentration (mmol/L)	Ion	Concentration (mmol/L)
Na^+	142	Cl^-	145
K^+	5.81	HPO_4^{2-}	0.778
Mg^{2+}	0.811	SO_4^{2-}	0.811
Ca^{2+}	1.26	HCO_3^-	4.17

2.9. Statistical Analysis

The data were statistically analyzed by one-way ANOVA analysis of variance and the Tukey test for multiple comparisons among the means at $p = 0.05$. The data were calculated with the help of Origin Pro 9.0 J (OriginLab Corp., Northampton, MA, USA).

3. Results

3.1. Morphology and Surface Roughness

Figure 2 shows SEM images of CA coating on each surface. No distinct differences were observed between 600 and 800 °C-2 h Y-TZP disks. Some small cracks were present on the outermost surface of apatite films. The presence of fused apatite crystal was observed on 1000 °C-2 h disks.

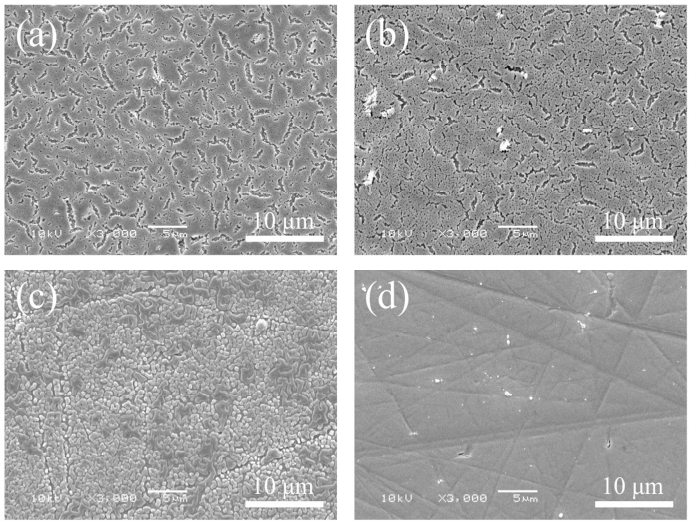

Figure 2. SEM images of the surfaces of (**a**) 600 °C-2 h, (**b**) 800 °C-2 h, (**c**) 1000 °C-2 h, and (**d**) 600 °C-4 h Y-TZP disks.

AFM images of each surface are shown in Figure 3. A difference in crystal size of coated CA was recognized. CA crystals with diameters approximately 100 nm were observed for 600 °C-2 h, and 150 nm for 800 °C-2 h. 1000 °C-2 h produced larger CA crystals with diameters of 500 nm, and 600 °C-4 h smaller CA crystals with diameters of 50 nm. Fused CA crystal was also identified by AFM observation, confirming the SEM observation.

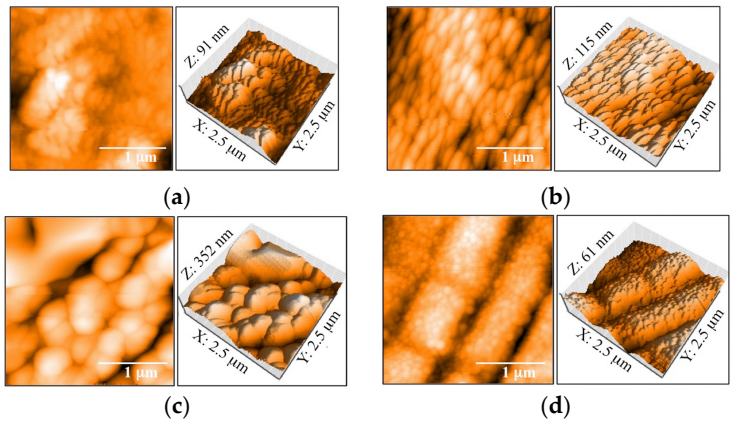

Figure 3. AFM images of CA crystals of (**a**) 600 °C-2 h, (**b**) 800 °C-2 h, (**c**) 1000 °C-2 h, and (**d**) 600 °C-4 h Y-TZP disks.

Surface roughness values obtained from AFM images are shown in Table 2. S_a and R_a for 1000 °C-2 h were significantly higher than those for 600 °C-2 h, 800 °C-2 h, and 600 °C-4 h ($p < 0.05$).

Table 2. Surface roughness (S_a and R_a values) of specimens.

Specimen	R_a (nm)	S_a (nm)
600 °C-2 h	10.31 (3.67) *	10.44 (2.94) *
800 °C-2 h	11.93 (3.84) *	11.12 (3.08) *
1000 °C-2 h	39.21 (5.71)	41.94 (4.85)
600 °C-4 h	6.49 (0.74) *	6.41 (0.85) *

Notes: Values in brackets are SD; * No significantly different at $p > 0.05$.

3.2. Surface Wettability

Contact angles against double distilled water are listed in Table 3. A significantly smaller contact angle was recognized for 800 °C-2 h disks compared with other heating conditions ($p < 0.05$).

Table 3. Contact angles against double-distilled water.

θ (°)	Specimen
41.89 ^{a} (4.42)	600 °C-2 h
18.14 (6.97)	800 °C-2 h
47.92 ^{a,b} (4.39)	1000 °C-2 h
51.37 ^{b,c} (2.80)	600 °C-4 h
56.73 ^{c} (2.96)	Non-Treated Y-TZP

Notes: Values in brackets are SD; ^{a,b,c} No significantly different at $p > 0.05$.

3.3. XRD Analysis of CA Coating Films

XRD patterns of CA coating films on Y-TZP disks at four different heating conditions are shown in Figure 4. Apatite structure was confirmed on all specimens. Peaks corresponding to

carbonate-containing apatite were observed at 2θ = 23.0°, 26.0°, 28.0°, 32.0°, 33.5°, 46.5°, and 49.5°, respectively. Greater intensities of the reflection of apatite peak were observed in 800 °C-2 h disks. Longer heating time e.g., 600 °C-4 h did not improve the crystallinity of CA coating film.

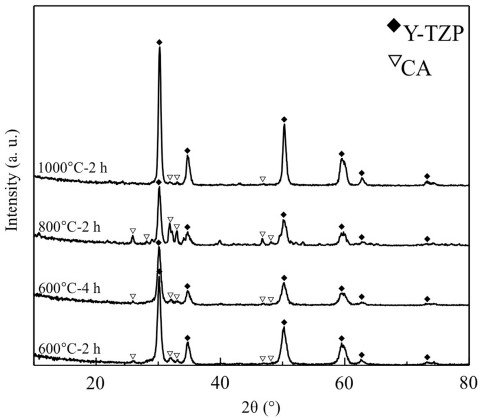

Figure 4. XRD patterns of CA films on the 600 °C-2 h, 800 °C-2 h, 1000 °C-2 h, and 600 °C-4 h Y-TZP disks. ♦: Y-TZP substrate, ▽: Carbonate apatite.

3.4. Adhesiveness of CA Coating Films

Table 4 shows L_c values obtained by the scratch test and Figure 5 shows panoramic images of the scratch trace and the images at the first crack in the coating in a representative sample. No significant differences were recognized in the L_c values among the four different samples ($p > 0.05$). The panoramic image of the scratch test revealed that clearer break down of the coating film was recognized at the position of the first crack for 600 °C-2 h and 600 °C-4 h than for 800 °C-2 h and 1000 °C-2 h disks.

Table 4. L_c values obtained by scratch test.

L_c Value (mN)	Specimen
169.96 (20.40)	600 °C-2 h
163.32 (16.09)	800 °C-2 h
176.67 (2.16)	1000 °C-2 h
150.56 (9.81)	600 °C-4 h

Note: Values in brackets are SD.

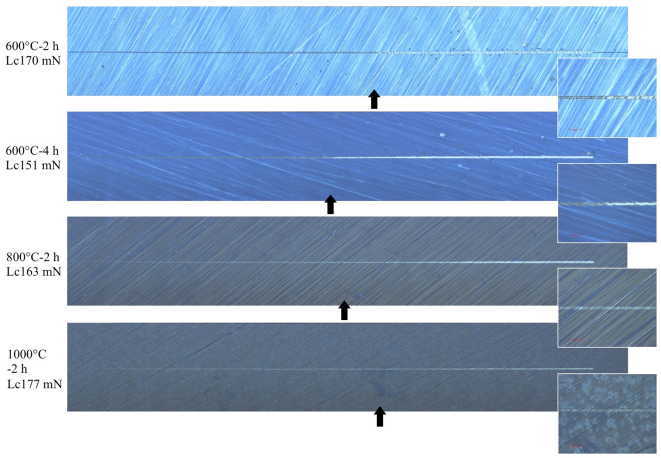

Figure 5. Panoramic images of the scratch trace and the images at the first crack in the coating of representative samples. Arrows: The first crack in the coating.

3.5. Durability of CA Coating Films

Figure 6 shows SEM images of the surfaces of CA coated Y-TZP disks after immersion in PBS. There are no distinct differences among the four different specimens. CA coating film was present after 30 days' immersion in PBS. A little pinhole was found on the surface of 1000 °C-2 h after 1 day immersion. Formation of slight cracks and pinholes was observed on all disks after 7 days' immersion in PBS. After 30 days' immersion, more crack formation was recognized along the scratches formed by polishing.

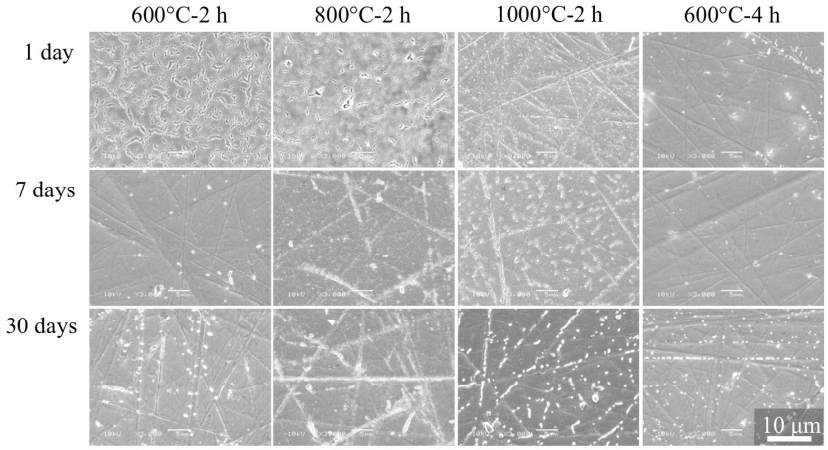

Figure 6. SEM images of the Y-TZP disks of four heating conditions after 1, 7, and 30 days of PBS immersion.

3.6. SBF Immersion

Figure 7 shows SEM images of the surfaces of CA coated Y-TZP disks from the four heating conditions after 24 and 48 h immersion in HBSS. Crystal deposition was observed on all surfaces of the CA coated Y-TZP disks after immersion in HBSS. After 48 h immersion, more growth of spherical crystals was observed on the surface of 600 °C-4 h and 800 °C-2 h Y-TZP disks and 800 °C-2 h Y-TZP disks showed a greater amount of spherical crystal precipitation.

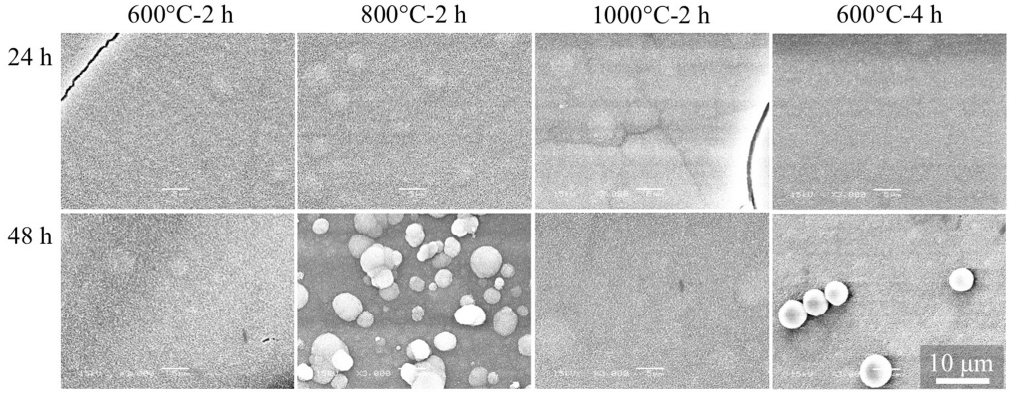

Figure 7. SEM images of the Y-TZP disks from four heating conditions after 24 and 48 h of HBSS immersion.

4. Discussion

In the present study, a CA coating was deposited on Y-TZP disks by using the molecular precursor method and the influence of heating conditions, temperature, and time, on the properties of the CA coated film was investigated. Four different heating conditions for CA coating were employed. Higher heating temperature did not produce more adherent and higher-crystallinity CA coatings. The null hypothesis was thus rejected.

Takahashi et al. [11] deposited a thin CA film on titanium using the molecular precursor method with various heating conditions from 300 to 700 °C for 2 h. Titanium is known to have a structural phase transition point at around 882 °C [14]. Moreover, higher heating temperatures than 700 °C caused oxidation of the titanium surface. Therefore, they concluded that a heating temperature of 600 °C is suitable for producing a CA film on titanium.

The structural phase transition point of Y-TZP is higher than that of titanium [17]. We expected that temperatures higher than 600 °C would produce more adherent and higher-crystallinity CA coatings on the Y-TZP surface. However, the adhesiveness of the CA coating film was not dependent on heating temperatures above 600 °C. XRD measurement indicated that higher crystallinity of CA coating was obtained with 800 °C heating but not by 1000 °C heating. The melting point of CA is reported to be approximately 1000 °C [18]. Thus, fusion of CA crystals deposited on Y-TZP occurred with 1000 °C heating as observed by SEM and AFM measurement, and some apatite crystals had an amorphous phase. As a result, the intensity of the reflection of the apatite peak after 1000 °C heating was weaker than that after 800 °C heating. On the contrary, the decrease in crystal size was observed when heat treatment at 600 °C was prolonged. Although the reason for the decrease in crystal size is not clear, it is presumed that the fusion of crystals did not proceed at 600 °C. Detailed studies about thermal behaviors of CA coating should be needed.

Although no significant differences were observed in the L_c values, there were differences in breakdown behaviors of CA coating films. 600 °C-2 h and 600 °C-4 h showed clearer breakdown at the first crack in the coating than 800 °C-2 h and 1000 °C-2 h. This was due to the difference in brittleness of CA coating films. Namely, 600 °C-2 h and 600 °C-4 h CA coating films may be more brittle than 800 °C-2 h and 1000 °C-2 h films. It is suggested that a higher heating temperature reduces the brittleness of CA coating films.

Many studies have reported the deposition of apatite on biomaterials after their immersion in SBF. It has been reported that the in vivo bioactivity of materials was shown to precisely mirror their in vitro apatite forming ability in SBF, namely, the more apatite that formed, the better the bone formation [19]. In the present study, HBSS was used as SBF. Hanawa and Ota [16] reported apatite layer deposition on a titanium surface after immersion in HBSS. Hayakawa and colleagues reported apatite deposition on biomaterials—such as thin-apatite coated titanium or titanium fiber, PLGA composite and DNA coated titanium—after immersion in SBF and found that better apatite deposition on the biomaterials in HBSS corresponded with better in vivo bone formation [12,13,20–22]. Our previous study also confirmed that better apatite deposition behavior of in vitro HBSS immersion experiment supported better in vivo bone formation on a CA-coated Y-TZP implant [9]. In the present study, greater amounts of apatite crystals deposited on the 800 °C-2 h surface after 48 h SBF immersion. Although the detailed reasons are not clear, it may be easier for epitaxial growth of deposited apatite on 800 °C-2 h to proceed with higher crystallinity. Animal experiments to elucidate the differences of CA coated Y-TZP at different heating conditions are needed in the near future. Moreover, Marrelli et al. [23] reported that surface roughness of zirconia strongly affected the mechanical strengths. Change of the mechanical strengths of Y-TZP after CA coating should be further investigated.

In clinical dentistry, demand for metal free implant system is increasing. Present apatite coating zirconia will be applicable for metal free implant system.

5. Conclusions

In this study, we evaluated the influence of heating conditions, heating temperature, and heating time, on the formation of a thin carbonate-containing hydroxyapatite (CA) film onto partially-stabilized zirconia using the molecular precursor method. A higher degree of crystallization of adherent CA coated film after 800 °C-2 h heating was recognized and greater amounts of apatite precipitation were identified by simulated body fluid immersion experiments. It was suggested that properties of CA coating on partially stabilized zirconia using a molecular precursor method were influenced by the heating temperature and time.

Acknowledgments: This work was supported by a Grant-in-Aid for Scientific Research (B) (15K20492), (17K17225) from the Japan Society for the Promotion of Science. The authors are grateful to Fumito Morigaki and Gwenael Bollore in Anton Paar Japan K.K. for the measurements of scratch test.

Author Contributions: Masatsugu Hirota performed apatite coating, surface observations, and characterization of CA coating; Chihiro Mochizuki and Mitsunobu Sato performed XRD analyses; Masatsugu Hirota performed durability testing and SBF immersion experiments; Chihiro Mochizuki and Mitsunobu Sato contributed materials; Masatsugu Hirota, Chihiro Mochizuki, and Tohru Hayakawa interpreted and discussed the results; Masatsugu Hirota and Tohru Hayakawa wrote the paper.

Conflicts of Interest: The authors declare no conflict of interest.

References

1. Pieralli, S.; Kohal, R.J.; Jung, R.E.; Vach, K.; Spies, B.C. Clinical outcomes of zirconia dental implants: A systematic review. *J. Dent. Res.* **2017**, *96*, 38–46. [CrossRef] [PubMed]
2. Özkurt, Z.; Kazazoğlu, E. Zirconia dental implants: A literature review. *J. Oral. Implantol.* **2011**, *37*, 367–376. [CrossRef] [PubMed]
3. Evans, A.G. Perspective on the development of high-toughness ceramics. *J. Am. Ceram. Soc.* **1990**, *73*, 187–206. [CrossRef]
4. Scarano, A.; Piattelli, M.; Caputi, S.; Favero, G.A.; Piattelli, A. Bacterial adhesion commercially pure titanium and zirconium oxide disks: An in vivo human study. *J. Periodontol.* **2004**, *75*, 292–296. [CrossRef] [PubMed]
5. Denry, I.; Kelly, J.R. State of the art of zirconia for dental applications. *Dent. Mater.* **2008**, *24*, 299–307. [CrossRef] [PubMed]
6. Bräunemark, P.I. Osseointegration and its experimental background. *J. Prosthet. Dent.* **1983**, *50*, 399–410. [CrossRef]
7. Hoffmann, O.; Angelov, N.; Gallez, F.; Jung, R.E.; Weber, F.E. The zirconia implant-bone interface: A preliminary histologic evaluation in rabbits. *Int. J. Oral. Maxillofac. Implant.* **2008**, *23*, 691–695.
8. Hoffmann, O.; Angelov, N.; Zafiropoulos, G.G.; Andreana, S. Osseointergration of zirconia implants with different surface characteristics: An evaluation in rabbits. *Int. J. Oral. Maxillofac. Implant.* **2012**, *27*, 352–358.
9. Hirota, M.; Hayakawa, T.; Ohkubo, C.; Sato, M.; Hara, H.; Toyama, T.; Tanaka, Y. Bone responses to zirconia implants with a thin carbonate-containing hydroxyapatite coating using a molecular precursor method. *J. Biomed. Mater. Res. Part B* **2014**, *102*, 1277–1288. [CrossRef] [PubMed]
10. Sato, M.; Hara, H.; Tomikoshi, H.; Mochizuki, C. Film fabrication of monolithic hydroxyapatite by an application of molecular precursor method. Proceedings of International Symposium on Advance Materials (ISAM/ISAT2), Islamabad, Pakistan, 23–27 September 2013.
11. Takahashi, K.; Hayakawa, T.; Yoshinari, M.; Hara, H.; Mochizuki, C.; Sato, M.; Nemoto, K. Molecular precursor method for thin calcium phosphate coating on titanium. *Thin Solid Films* **2005**, *484*, 1–9. [CrossRef]
12. Hayakawa, T.; Takahashi, K.; Okada, H.; Yoshinari, M.; Hara, H.; Mochizuki, C.; Yamamoto, H.; Sato, M. Effect of thin carbonate-containing apatite (CA) coating of titanium fiber mesh on trabecular bone response. *J. Mater. Sci. Mater. Med.* **2008**, *19*, 2087–2096. [CrossRef] [PubMed]
13. Amemiya, T.; Fukayo, Y.; Nakaoka, K.; Hamada, Y.; Hayakawa, T. Tissue response of surface modified three dimensional titanium fiber structure. *J. Hard Tissue Biol.* **2014**, *23*, 137–148. [CrossRef]
14. Pushkareva, M.; Adrien, J.; Marie, E.; Segurado, J.; Llorca, J.; Weck, A. Three-dimensional investigation of grain orientation effects on void growth in commerciall pure titanium. *Mater. Sci. Eng. A* **2016**, *671*, 221–232. [CrossRef]
15. Steinmann, P.A.; Tardy, Y.; Hintermann, H.E. Adhesion testing by the scratch test method: The influence of intrinsic and extrinsic parameters on the critical load. *Thin Solid Films* **1987**, *154*, 333–349. [CrossRef]
16. Hanawa, T.; Ota, M. Calcium phosphate naturally formed on titanium in electrolyte solution. *Biomaterials* **1991**, *12*, 767–774. [CrossRef]
17. Garvie, R.C.; Hannink, R.H.; Pascoe, R.T. Ceramic steel? *Nature* **1975**, *258*, 703–704. [CrossRef]
18. Rohanizadeh, R.; LeGeros, R.Z.; Fan, D.; Jean, A.; Daculsi, G. Ultrastructural properties of laser-irradiated and heat-treated dentin. *J. Dent. Res.* **1999**, *78*, 1829–1835. [CrossRef] [PubMed]
19. Kokubo, T.; Takamada, H. How useful is SBF in predicting in vivo bone bioactivity? *Biomaterials* **2006**, *27*, 2907–2915. [CrossRef] [PubMed]

20. Mochizuki, C.; Sasaki, Y.; Hara, H.; Sato, M.; Hayakawa, T.; Yang, F.; Hu, X.; Shen, H.; Wang, S. Crystallinity controlled apatites through a Ca-EDTA complex and their porous composites with PLGA. *J. Biomed. Mater. Res. Part B* **2009**, *90*, 290–301.
21. Hayakawa, T.; Mochizuki, C.; Hara, H.; Sato, M.; Yang, F.; Shen, H.; Wang, S. In vivo evaluation of composites of PLGA and apatite with two different levels of crystallinity. *J. Mater. Sci. Mater. Med.* **2010**, *21*, 251–258. [CrossRef] [PubMed]
22. Sakurai, T.; Yoshinari, M.; Toyama, T.; Hayakawa, T.; Ohkubo, C. Effects of a multilayered DNA/protamine coating on titanium implants on bone responses. *J. Biomed. Mater. Res. Part A* **2016**, *104*, 1500–1509. [CrossRef] [PubMed]
23. Marrelli, M.; Maletta, C.; Inchingolo, F.; Alfano, M.; Tatullo, M. Three-point bending tests of zirconia core/veneer ceramics for dental restorations. *Int. J. Dent.* **2013**, *2013*, 831976. [CrossRef] [PubMed]